A Library of Protein Cage Architectures as Nanomaterials

M.L. Flenniken (✉), M. Uchida, L.O. Liepold, S. Kang, M.J. Young, T. Douglas

Contents

Abstract Virus capsids and other structurally related cage-like proteins such as ferritins, dps, and heat shock proteins have three distinct surfaces (inside, outside, interface) that can be exploited to generate nanomaterials with multiple functionality by design. Protein cages are biological in origin and each cage exhibits extremely homogeneous size distribution. This homogeneity can be used to attain a high degree of homogeneity of the templated material and its associated property. A series of protein cages exhibiting diversity in size, functionality, and chemical and thermal stabilities can be utilized for materials synthesis under a variety of conditions. Since synthetic approaches to materials science often use harsh temperature and pH, it is an advantage to utilize protein cages from extreme environments. In this chapter, we review recent studies on discovering novel protein cages from harsh natural environments such as the acidic thermal hot springs at Yellowstone National Park (YNP) and on utilizing protein cages as nano-scale platforms for developing nanomaterials with wide range of applications from electronics to biomedicine.

M.L. Flenniken
University of California, San Francisco, Microbiology and Immunology Department, 600 16th Street, Genentech Hall S576, Box 2280, San Francisco, CA 94158–2517, USA
e-mail: michelle.flenniken@ucsf.edu

M. Manchester, N.F. Steinmetz (eds.), *Viruses and Nanotechnology*,
Current Topics in Microbiology and Immunology 327.

Abbreviations CCMV Cowpea chlorotic mottle virus, Dps DNA-binding proteins from starved cells, Dps-L Dps-like protein, Hsp Heat shock protein, MRI Magnetic resonance imaging, STIV *Sulfulobus* turreted icosahedral virus, TMV Tobacco Mosaic Virus, YNP Yellowstone National Park

Introduction

In nature, proteins orchestrate the formation of elaborate inorganic structures, for example, the single-celled algae, *Emiliania huxleyi*, form intricate calcium carbonate ($CaCO_3$) structures called coccoliths (Fig. 1a) (Wikipedia 2005). In comparison, synthetic preparations of $CaCO_3$ result in a far more limited range of morphologies. Coccolith formation is controlled by proteins that direct the assembly of crystallites into intricate 3D assemblies. The degree of control exhibited by this and other natural systems is an inspiration for materials scientists.

Viral capsids are also naturally occurring, intricate assemblies that serve to house, protect, and deliver nucleic acid genomes to specific host cells. Therefore, their structures must be robust enough to survive diverse conditions, yet sufficiently dynamic to release their genome into host cells. Proteins are the building blocks of viral capsids; therefore, protein–protein interactions dictate their 3D structure. Typically, protein motifs on the interior are involved in packaging nucleic acid, whereas those on the exterior are involved with cell recognition and attachment. Viral capsids devoid of their nucleic acid genomes can be thought of as nanocontainers. The diversity of these nanocontainers is seemingly endless, since viruses are ubiquitous with life. In our investigations of archaeal viruses found in the acidic hot (>90°C) springs of Yellowstone National Park (YNP), we discovered and structurally characterized the *Sulfolobus* turreted icosahedral virus (STIV), which presents elaborate turret-like structures on its exterior (Rice et al. 2001, 2004; Synder et al. 2003) (Fig. 1b).

Both the coccolith and archaeal virus are examples of naturally occurring 3D assemblies whose architecture is dictated by proteins. Inspired by nature, we have selected a bio-mimetic approach to nanomaterials synthesis that is bioassisted. We utilize protein cage architectures to serve as size-constrained reaction vessels and chemical building blocks (Douglas and Young 1998, 1999; Douglas et al. 2002b, 2004; Flenniken et al. 2004; Kelm et al. 2005b).

Protein cage architectures, 10–100 nm in diameter, are self-assembled hollow spheres derived from viruses and other biological cages, including heat shock proteins (Hsp), DNA-binding proteins from starved cells (Dps), and ferritins. These architectures play critical biological roles. For example, heat shock proteins are thought to act as chaperones that prevent protein denaturation, and ferritins are known to store iron (which is both essential and toxic) as a nanoparticle of iron oxide (Harrison and Arosio 1996; Narberhaus 2002). While each of these structures has evolved to perform a unique natural function, they are similar in that they are all essentially proteinaceous containers with three distinct surfaces (interior, exterior, and subunit interface) to which one can impart function by design. Protein cage architectures have demonstrated

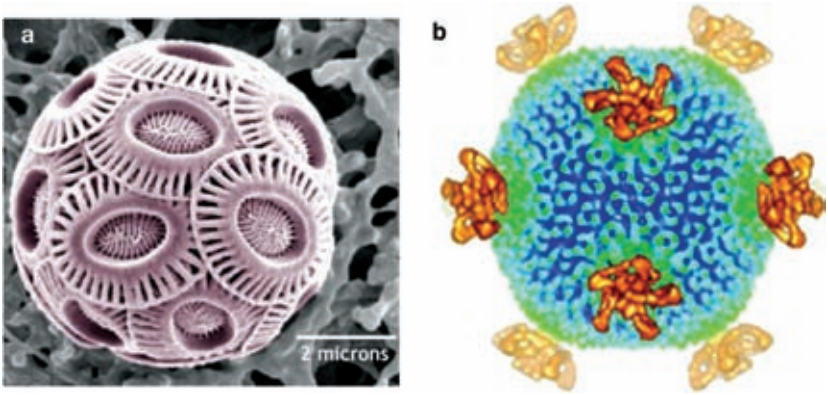

Fig. 1a,b Biological assemblies. **a** *Emiliania huxleyi* formed $CaCO_3$ coccolith structures arranged in a coccosphere, ~6 mM in diameter. (Used with permission from the Wikipedia:Free Encyclopedia (http://en.wikipedia.org, with permission; picture by Dr. Markus Geisen) **b** Cryo-TEM image reconstruction of the ~74-nm-diameter STIV capsid with turret-like projections extending from each of the fivefold vertices. (Rice et al. 2004, with permission)

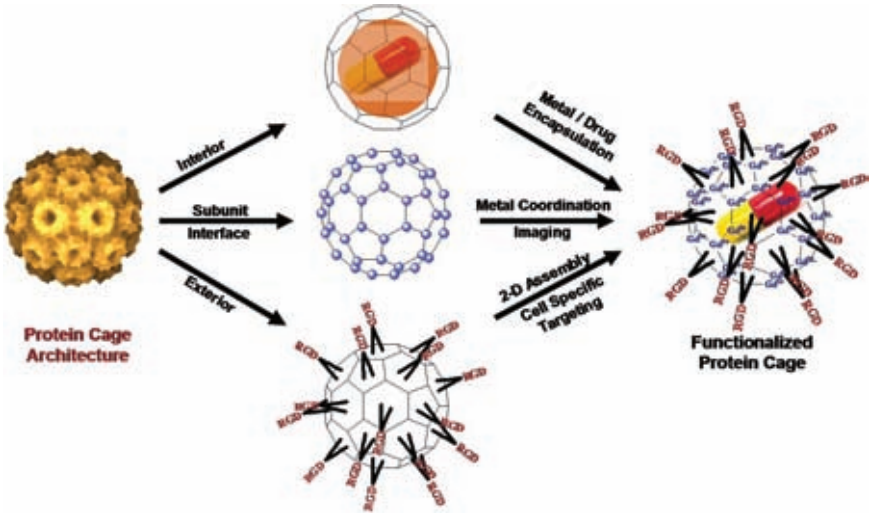

Fig. 2 Schematic representation of protein cage functionalization. Protein cage architectures have three surfaces (interior, subunit interface, and exterior) amenable to both genetic and chemical modification. (Mark Allen)

utility in nanotechnology with applications including inorganic nanoparticle synthesis and the development of targeted therapeutic and imaging delivery agents (Allen et al. 2002, 2003, 2005; Bulte et al. 1994a, 1994b, 2001; Chatterji et al. 2002, 2004a, 2004b; Douglas and Stark 2000; Flenniken et al. 2005, 2006; Gillitzer et al. 2002; Hikono et al. 2006; Liepold et al. 2007; Raja et al. 2003a, 2003b; Schlick et al. 2005; Wang et al. 2002a, 2002b, 2002c) (Fig. 2).

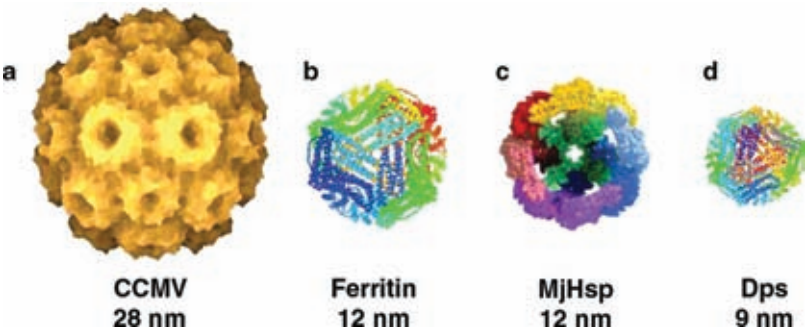

Fig. 3a–d Protein cage library. **a** Cowpea chlorotic mottle viral (CCMV) capsid cryo-image reconstruction. (Reddy et al. 2001, with permission from VIPER). **b** Ribbon diagram of human H-chain ferritin; our library also includes horse spleen and *Pyrococcus furiosus* ferritins. **c** Small heat shock protein (Hsp) from *Methanococcus jannaschii.* (Kim et al. 1998a, with permission). **d** Ribbon diagram of Dps (DNA binding protein from starved cells) protein, our library includes a Dps protein from *Listeria innocua* and Dps-like proteins from *Sulfolobus solfataricus* and *Pyrococcus furiosus*

Protein cage architectures are naturally diverse; each has unique attributes (including size, structure, solvent accessibility, chemical and temperature stability, structural plasticity, assembly and disassembly parameters, and electrostatics) useful to particular applications. Importantly, one can capitalize on these features or alter them via genetic or chemical modification. Atomic level structural information identifies the precise location of amino acids within protein cage architectures and in turn allows for the rational inclusion, exclusion, and substitution of amino acid(s) (at the genetic level) resulting in protein cages with novel functional properties.

In this work, we review recent strides our lab has taken toward the development of protein cage architectures as nanomaterials for bioengineering and biomedicine. We have developed a library of protein cages (including Cowpea chlorotic mottle virus [CCMV], ferritin, Hsp, and Dps) as size-constrained reaction vessels and as platforms for genetic and chemical modification (Fig. 3). This protein cage library consists of a small sampling of the great diversity of naturally available protein cage architectures. Utilization of protein cages for applications in nanotechnology often requires their use in harsh synthetic conditions. Therefore, we have focused some of our efforts on novel protein cage discovery from harsh natural environments.

Protein Cage Discovery from Hyperthermophilic Archaea

The quest to find new, potentially stable protein cages has led our group to the hot springs of Yellowstone National Park. Within these extreme environments (pH 1.5–5.5; temperature range of 70°C to >100°C), organisms in the archaeal domain such as *Sulfolobus solfataricus* are well represented (Rice et al. 2004). *Sulfolobus* and other hyperthermophiles serve as hosts for novel and largely uncharacterized viruses. Of

the approximately 5,100 known viruses, only 36 archaeal viruses, or virus-like particles, have been described to date (International Committee on Taxonomy of Viruses, http://www.ncbi.nlm.nih.gov/ICTVdb/Ictv/index.htm (Ackerman 2001). Prior to our investigation, no viruses of *Sulfolobus* from YNP had been described (Rice et al. 2004). In 2001, we reported six unique particle morphologies isolated from YNP, three of which were similar to viruses isolated from Iceland or Japan and the other three exhibited novel morphologies (Rice et al. 2001) (Fig. 4). One YNP virus, named

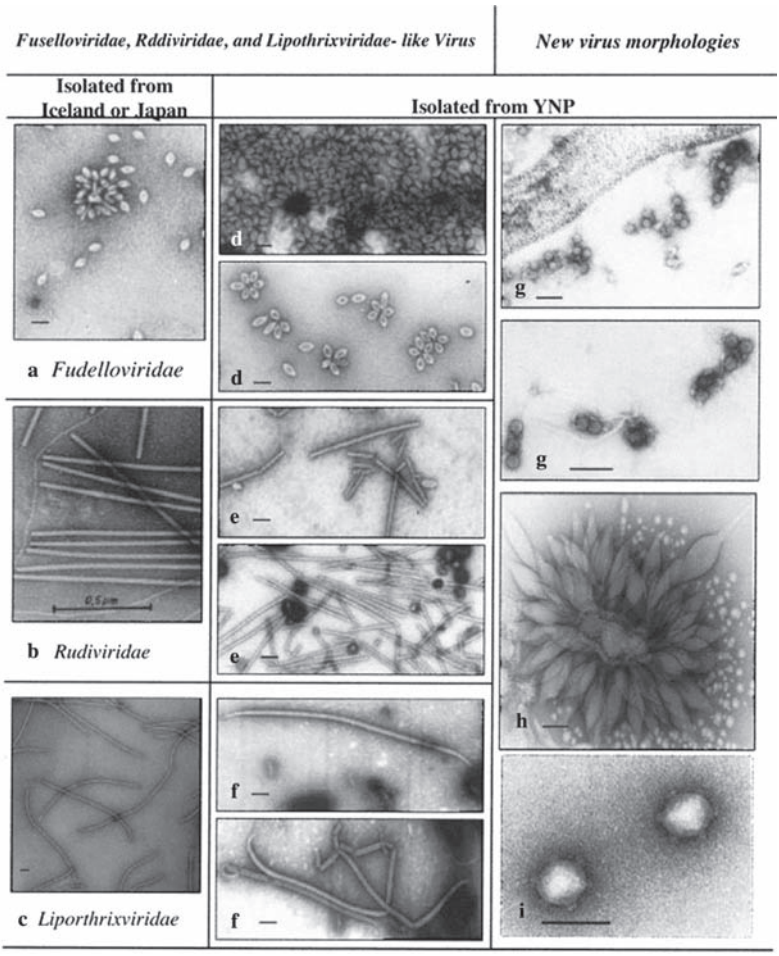

Fig. 4a–i Transmission electron micrographs of virus and virus-like particles from YNP. **a** SSV1 Fusellovirus, **b** SIRV Rudivirus, and **c** SIFV Lipothrixvirus previously isolated from thermal areas of Japan or Iceland (courtesy of W. Zillig, Max-Planck Institut für Biochemie, Martinsried, Germany). **d** SSV-like, **e** SIRV-like, and **f** SIFV-like particle morphologies isolated from YNP thermal features. **g–i** Virus-like P articles isolated from YNP thermal features. Bars indicate 100 nm. (Rice et al. 2001, with permission)

STIV, has an approximately 74-nm diameter capsid from which turret-like projections extend (Rice et al. 2004) (Fig. 1b). The pseudo-T=31 structure of STIV is unique. A structural comparison of STIV, bacterial phage PRD1, and human adenovirus revealed tertiary and quaternary structural similarities suggestive of a common ancestry that predates the division of life into three domains (Eukarya, Bacteria, and Archaea) more than 3 billion years ago (Rice et al. 2004).

In addition to new viruses, hyperthermophilic organisms are hosts to other protein cage architectures, including Hsp cages, ferritins, Dps and Dps-like proteins. Genome sequencing of many archaea since the first, *Methanococcus jannaschii* (isolated from a 2,600-μ-deep hydrothermal vent in the Pacific Ocean) in 1996 has aided the discovery and study of protein cages (Bulte et al. 1996). The small heat shock protein from *M. jannaschii* (*Mj*Hsp) assembles into a 12-nm-diameter cage with octahedral symmetry (Kim et al. 1998a, 1998b) (Fig. 3). The crystal structure of this hollow spherical complex determined that there are eight triangular and six square pores that allow free exchange between the interior and bulk solution, a useful feature for applications in nanotechnology, including loading therapeutics into protein cage architectures (Flenniken et al. 2003, 2005; Kim et al. 1998a).

Utilizing genomic information, our lab recently identified Dps-like protein cages from *Sulfolobus solfataricus* (*Ss*Dps-L) and *Pyrococcus furiosus* (*Pf*Dps-L) (Maeder et al; 1999; Ramsay et al. 2006; Wiedenheft et al. 2005). Characterization of the *Ss*Dps-L determined that it serves to protect *S. solfataricus* against oxidative stress and in the process mineralizes a nanoparticle of iron oxide within its cage structure (Ramsay et al. 2006; Wiedenheft et al. 2005). The *Ss*Dps-L protein was identified based on predicted secondary and tertiary structural similarity to a Dps protein from *Listeria innocua*, while the *Pf*Dps-L has a very high sequence homology to the *Ss*Dps-L (Su et al. 2005; Wiedenheft et al. 2005). These 9.7-nm-diameter protein cages self-assemble from 12 protein monomers and represent the smallest of the protein cages in our library (Ramsay et al. 2006; Wiedenheft et al. 2005) (Fig. 5).

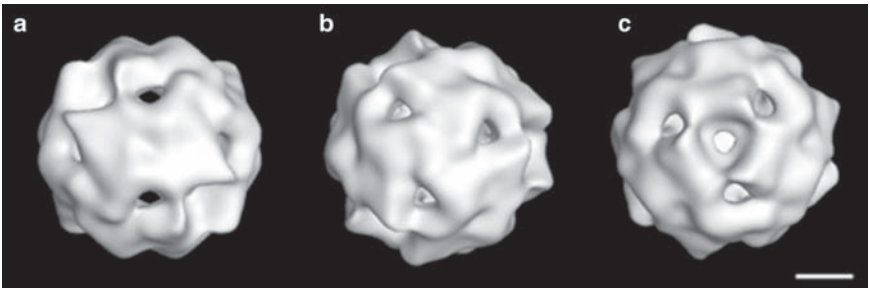

Fig. 5a–c 3D image reconstruction of the assembled *Ss*Dps-L cage. Surface-shaded views of reconstructed negative-stained images displayed along the (**a**) twofold (2F) axis, and (**b** and **c**) along the two nonequivalent environments at each end of the threefold (3F) axis. Scale bar: 2.5 nm. (Wiedenheft et al. 2005, with permission)

Protein Cages from Mesophilic Organisms

Protein cages isolated from thermophilic environments are desirable as building blocks for nanotechnology due to their potential stability in harsh reaction conditions including high temperature and pH extremes. Interestingly, one of the most stable protein cage architectures, ferritin, is commonly found in mesophilic organisms, including animals, plants, and microbes. For example, horse spleen ferritin exhibits broad pH (pH 2–8) and temperature stability (<70°C). Ferritins are involved in iron sequestration, which they accomplish through the oxidation of soluble Fe(II) using O_2 (Chasteen and Harrison 1999; Harrison and Arosio 1996). This oxidation results in the formation of a nanoparticle of Fe_2O_3 encapsulated (and rendered nontoxic) within the protein cage. High charge density on the inner surface of the protein cage promotes this reaction, which is assisted by an enzymatic (ferroxidase) activity in some ferritin subunits (Chasteen and Harrison 1999; Douglas and Riipoll 1998; Harrison and Arosio 1996). Ferritins are made up of 24 subunits, which form a spherical cage 12 nm in diameter (Harrison et al. 1976; Harrison and Arosio 1996). The ferritin family also includes the 24 subunit bacterioferritins and the Dps class of proteins, which assemble from 12 monomers. We, and others, have employed ferritin and Dps cage architectures for mineralization of inorganic nanoparticles (Allen et al. 2002, 2003; Douglas 1996; Douglas and Stark 2000; Ensign et al. 2004; Hosein et al. 2004; Wiedenheft et al. 2005). Recently, we utilized a genetically modified recombinantly expressed human H-chain ferritin as a platform for cell-specific delivery of imaging agents in vitro (Uchida et al. 2006).

Mesophilic viral capsids have also exhibited utility for applications in nanotechnology (Allen et al. 2005; Chatterji et al. 2002, 2004a, 2004b, 2005; Douglas and Young 1998, 1999; Douglas et al. 2002a; Flenniken et al. 2004; Gillitzer et al. 2002; Klem et al. 2003; Liepold et al. 2007; Mao et al. 2003, 2004; Raja et al. 2003a, 2003b; Schlick et al. 2005; Strable et al. 2004; Wang et al. 2002a, 2002b, 2002c). We have routinely employed the CCMV capsid as a scaffold for chemical conjugation of biologically important molecules, including imaging agents (fluorescein, Texas red, gadolinium chelators), and as a size-constrained reaction vessel for mineralization of metallic and metal oxide nanoparticles (Douglas and Young 1998; Gillitzer et al. 2002; Klem et al. 2003; Liepold et al. 2007). The CCMV capsid assembles from 180 copies of a single protein into a 28-nm icosohedral shell (Johnson and Speir 1997; Speir et al. 1995; Shao et al. 1995). Wild type and genetically engineered CCMV capsids are purified from both the natural cowpea plant host and a yeast heterologous expression system (Brumfield et al. 2004).

Protein Cages for Inorganic Nanoparticle Synthesis

In our initial work, CCMV capsids were employed for the mineralization of polyoxometalate species (paratungstate and decavanadate) (Douglas and Young 1998). The virion's interior cavity constrains mineral growth, resulting in a spherical

nanoparticle with a maximum diameter of approximately 24 nm (Douglas and Young 1998). The exterior and interior of the CCMV capsid are chemically distinct environments. The interior surface is more positively charged than the exterior, thus allowing it to serve as a nucleation site for aggregation of anionic precursors and crystal growth. After nucleation, the size and shape of the mineral are defined by the interior of the virion. In addition to the endogenous properties of size, shape, and delineation of charge on the interior and exterior surfaces, the CCMV viral capsid undergoes a pH-dependant structural transition (gating) (Schneemann and Youg 2003; Speir et al. 1995). This pH-dependant reversible gating or swelling is a structural change of the virus capsid that results in a 10% increase of viral dimension at pH greater than 6.5 in the absence of metal cations (at pH <6.5 the virion is in its closed confirmation) (Speir et al. 1995). During the polyoxometalate mineralization reaction, the pH was lowered entrapping the mineral within the viral capsid (Douglas and Young 1998).

In addition to utilizing the inherent properties of the CCMV protein cage as described above, we can dramatically change these properties via genetic engineering. Specifically, site-directed polymerase chain reaction-mediated mutagenesis is employed to alter the DNA encoding the viral capsid protein. Protein expression results in the replacement of wild type amino acids and functional groups with novel functional groups at precisely defined locations due to the quaternary structure of the virion. Additionally, genetic modifications allow for the introduction of novel peptide sequences as extensions from the N- and C-termini or within the loop regions of the subunit structure (Liepold et al. 1983).

Inspired by the iron storage protein cage, ferritin, and its ability to mineralize iron oxide nanoparticles in a size-constrained fashion, we constructed the subE mutant of CCMV. SubE was made by replacing eight of the positively charged amino acid residues (5-Arg, 3-Lys) on the N-terminus of the protein with negatively charged glutamic acids (Glu). This created a cage with a negatively charged interior, illustrating the plasticity of the CCMV cage toward genetic manipulation (Brumfield et al. 2004; Douglas et al. 2002b). The electrostatically altered viral protein cages did not differ in overall structure from wild type CCMV, but they exhibited different mineralization capabilities (Brumfield et al. 2004). SubE's negatively charged interior promoted interaction with cationic Fe(II) ions and subsequent oxidative hydrolysis led to the formation of approximately 24-nm particles of lepidocrocite (γ-FeOOH) constrained within the interior cavity of the protein cage (Douglas et al. 2002b).

We have developed the library of protein cages available for biomineralization and chemical derivatization to include many protein cage architectures of both viral and nonviral origin. Protein cage architectures housing iron oxide (magnetite) have potential to serve in magnetic memory storage and as contrast agents for magnetic resonance imaging (MRI). In addition to CCMV and ferritin, we have mineralized iron oxide nanoparticles within a number of additional protein cages. These include the Dps protein cage from *Listeria innocua* (*Li*Dps), the *Ss*Dps-L cage from *S. solfataricus*, the small Hsp (*Mj*Hsp) cage from *M. jannaschii*, the ferritin cage from horse spleen, human H-chain ferritin and the ferritin from the hyperthermophile

Pyrococcus furiosus (Allen et al. 2002, 2003; Douglas and Mann 1995; Flenniken et al. 2003; Klem et al. 2005b; Parker et al. 2008; Uchida et al. 2006; Wiedenheft et al. 2005). The *Li*Dps was shown by others to mineralize Fe as a nanoparticle of an as-yet unidentified ferric oxyhydroxide (Stefanini et al. 1999; Yang et al. 2000). We utilized the *Li*Dps cage as a size-constrained reaction vessel for Fe_3O_4 mineralization under the nonphysiologic conditions of elevated pH and temperature (pH 8.5, 65°C) and in the presence of substoichiometric amounts of oxidant (H_2O_2) (Allen et al. 2002). Under these conditions, with 400 Fe(II) per cage, ferrimagnetic nanoparticles of Fe_3O_4 (4 nm in diameter) formed inside the *Li*Dps cage (Allen et al. 2002) (Fig. 6).

Analogous to ferritin and *Li*Dps protein cages, the *Mj*Hsp cage has been shown to act as a size-constrained reaction vessel for the formation of iron oxide (ferrihydrite). Transmission electron microscope imaging of the 9-nm cores within Hsp cages, as compared to iron oxide formation in the absence of protein cages, underscore the importance of the protein cage to control and constrain mineral growth (Flenniken et al. 2003) (Fig. 7). Like iron oxide formation in the CCMV SubE protein cage, mineralization within the Hsp cage illustrates the ability of many protein cage platforms to function similarly as nanocontainers for biomineralization.

Based on the structural similarity of *Ss*Dps-L to the Dps protein from *L. innocua*, we explored the in vitro mineralization capability of the 10-nm-diameter *Ss*Dps-L protein cage (Wiedenheft et al. 2005). This analysis revealed that unlike ferritins, *Ss*Dps-L mineralizes iron oxide more efficiently in the presence of H_2O_2 as compared to ferritins that catalyze Fe(II) oxidation with O_2. Ferritin protein cages are thought to serve as iron storage proteins, whereas Dps and Dps-like proteins mineralize iron as a consequence of hydrogen peroxide reduction, therefore serving as antioxidants that protect the organism during oxidative stress (Wiedenheft et al. 2005).

In addition to polyoxometalates and iron oxides, we and others have expanded the range of inorganic nanoparticles formed within these architectures to include important semiconducting materials (Klem et al. 2005b). Ferritin architectures have

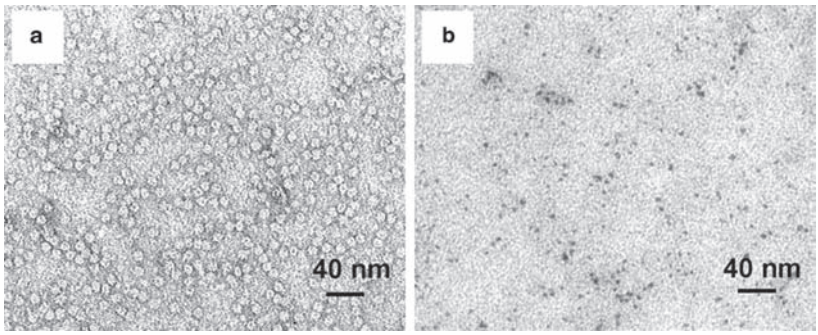

Fig. 6a, b Transmission electron micrographs of mineralized *L. innocua* Dps cage. *Li*Dps mineralized with g-Fe2O3 (**a**) stained with uranyl acetate and (**b**) unstained. (Allen et al. 2002, with permission)

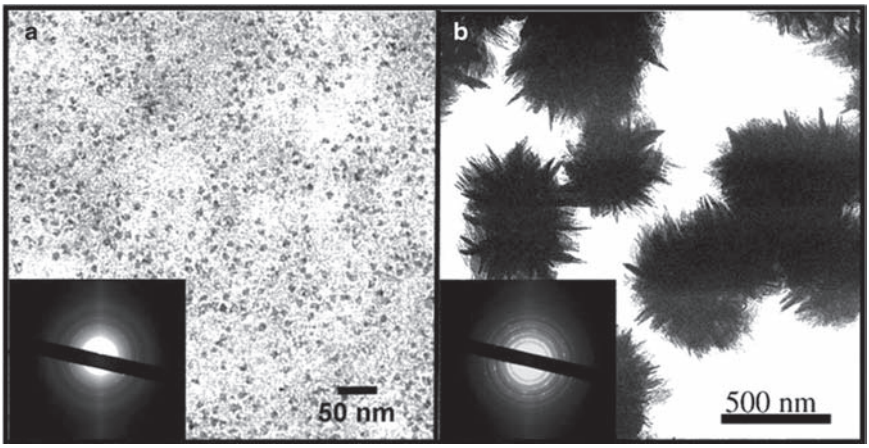

Fig. 7a, b Transmission electron micrographs of iron oxide mineralization. **a** Iron oxide cores inside Hsp cages; scale bar, 50 nm. **b** TEM of control sample illustrating the bulk precipitation of iron oxide in the absence of Hsp protein cages; scale bar, 500 nm. The insets show the electron diffraction from each sample. (Flenniken et al. 2003, with permssion)

been utilized as a constrained template for the synthesis of CoPt, FePt, ZnSe, Pd, CdS, Ag, and Eu_2O_3 nanoparticles (Allen et al. 2002, 2003; Douglas and Stark 2000; Douglas et al. 2002b; Klem et al. 2005a, 2005b, 2008; Varpness et al. 2005). *Li*Dps served as a size-constrained reaction vessel for the synthesis of two cobalt oxide minerals (Co_3O_4 and Co(O)OH) (Allen et al. 2003). In addition, utilizing the heat shock protein architecture, we have made CoPt and Pt nanoparticles (Klem et al. 2005a; Varpness et al. 2005). Inorganic nanoparticles templated by protein cages have been utilized in the fabrication of semiconducting devices. Yamashita and colleagues have developed what has been called the bionano process (BNP) for the fabrication of metal-oxide-semiconductor (MOS) such as a floating nanodot gate memory device or low-temperature polycrystalline silicon thin film transistor flash memory (Hikono et al. 2006; Ichikawa et al. 2007; Matsui et al. 2007; Miura et al. 2006; Yamada et al. 2007). The performance and characteristics of the MOS devices depend on the size, shape, and density of the nanodot array. They have recently demonstrated that the BNP allows control of these three parameters (Yamada et al. 2007).

Biomimetic approaches to materials synthesis have explored the interaction between proteins and minerals at their interface. Pioneering work by A. Belcher's group utilized the phage display library technique (originally developed to determine peptide–protein interactions for mapping antibody–antigen binding sites) to identify peptides that bound inorganic substrates normally not encountered by biological systems (Belcher et al. 2001; Burritt et al. 1996; Mao et al. 2004; Scott and Smith 1990; Seeman and Belcher 2002; Smith and Petrenko 1997; Whaley et al. 2000). In turn, when these peptides were present in mineralization reactions they directed the

growth of specific crystal phases (Mao et al. 2004). The KTHEIHSPLLHK peptide specifically binds the $L1_0$ phase of CoPt (Mao et al. 2004). Genetic incorporation of this CoPt-binding peptide into the *Mj*Hsp cage interior (CP-Hsp) enabled phase-specific nucleation and size-constrained formation of CoPt nanoparticles with an average diameter of 6.5 nm (Klem et al. 2005a). The metallized CP-Hsp exhibited room temperature ferromagnetism, whereas HspG41C, a genetic variant of *Mj*Hsp with an internal cysteine, did not because of the nonspecific ordering of the CoPt mineral within its interior (Flenniken et al. 2003; Klem et al. 2005a). These results underscore the ability of specific peptide sequences to direct mineral formation. Protein cage architectures that incorporate these sequences (either inherently or because of genetic manipulation) are more than nanocontainers that serve as size-constrained reaction vessels. Their specific amino acids play a critical role in mineral formation in a manner that is not yet completely understood. By developing protein cage platforms for nanomaterial synthesis, we hope to gain insight into the mechanisms by which proteins direct mineral formation.

In addition to serving as size-constrained reaction vessels, protein cage architectures have been used as a scaffold to construct unique catalysts (Endo et al. 2007; Ensign et al. 2004; Kim et al. 2002; Miller et al. 2007; Nkere et al. 1997; Varpness et al. 2005). Native ferrihydrite-containing ferritins were utilized to catalyze the photoreduction of toxic Cr(VI) species to Cr(III) (Kim et al. 2002). In addition, ferrihydrite-containing ferritins were employed as catalysts for the photoreduction of Cu(II) to form colloidal Cu(0) nanoparticles ranging in size from 4 to 31 nm (Ensign et al. 2004). Treatment of iron and cobalt oxide containing ferritin protein cages with H_2 at elevated temperature resulted in conversion to the metallic Fe or Co nanoparticles without loss of morphology (Hosein et al. 2004). The catalytic activity of these highly reactive nanoparticles is being explored. Recently, TMV has been used as a scaffold to mimic light harvesting systems (Endo et al. 2007; Miller et al. 2007). Porphyrin complexes (Endo et al. 2007) or fluorescent chromophores (Miller et al. 2007) were attached in a spatially defined manner onto the inner surface of the TMV particles. Efficient energy transfer, from large numbers of donor chromophores to a single acceptor, has been demonstrated (Endo et al. 2007; Miller et al. 2007). For direct hydrogen production, Hsp cages were utilized as a template for Pt nanoparticle synthesis (Varpness et al. 2005). The Pt nanoparticles contained within Hsp exhibited comparable catalytic hydrogen production activity to hydrogenase enzymes (Varpness et al. 2005). Initial hydrogen production rates for this system were approximately tenfold greater than previously reported values from Pt colloids (Varpness et al. 2005).

The examples described thus far demonstrate the utility of protein cage architectures for inorganic nanomaterials synthesis and catalysis. In addition, metal-containing protein cages have potential medical applications. Protein cage architectures housing iron oxide (magnetite) nanoparticles have potential medical applications in imaging, serving as MRI contrast agents, and in cancer treatment by hyperthermia (Allen et al. 2002; Butle et al. 1994; Kawashita et al. 2005; Klem et al. 2005b; Luderer et al. 1983).

Protein Cages for Medical Imaging

We have developed protein cage platforms with fluorescence and MRI capabilities. Imaging capabilities were imparted via (1) magnetite mineralization within cage interiors, (2) utilization of endogenous sites to bind paramagnetic metal ions, (3) genetic incorporation of metal chelating peptides, and (4) chemical modifications, including covalently binding fluorophores and gadolinium chelators (Allen et al. 2002, 2005; Basu et al. 2003; Flenniken et al. 2003, 2005; Gillitzer et al. 2002; Liepold et al. 2007).

The road to developing the CCMV viral capsid as an MRI contrast agent has involved utilization of the endogenous properties of the cage, as well as both genetic and chemical modification. CCMV naturally coordinates divalent calcium (Ca^{2+}) ions at its quasi-threefold axis, but in vitro other metal ions, including paramagnetic gadolinium (Gd^{3+}), can bind these sites (Allen et al. 2005; Basu et al. 2003). The CCMV capsid is composed of 180 subunits, each of which binds a Gd^{3+} ion resulting in a particle with a high Gd^{3+} payload and in turn high relaxivity values (Allen et al. 2005). The T_1 and T_2 ionic relaxivities of water protons, as measured at 61 MHz, were 202 and 376 $mM^{-1}s^{-1}$, respectively; these are the highest values reported for a molecular paramagnetic material to date (Allen et al. 2005). Although Gd-CCMV exhibited high relaxivity values, the dissociation constant (K_d) for Gd^{3+} is 31 μM, insufficient for in vivo applications (Allen et al. 2005. In order to increase the binding affinity, we genetically incorporated the metal-binding motif from calmodulin into the CCMV architecture (Le Clainche et al. 2003; Liepold et al. 2007). At the same time, we explored the chemical attachment of GdDOTA onto endogenous lysines on CCMV. Although these two approaches both substantially increased the affinity for Gd^{3+}, there was a loss of relaxivity efficiency in both cases, as compared to Gd^{3+} bound to the endogenous binding sites of CCMV. The loss of relaxivity likely stems from two sources. First, in the case of the endogenous metal-binding sites of CCMV, there is more than one water molecule bound to Gd^{3+} (a higher number of Gd^{3+}-bound water molecules is preferred for efficient relaxivity properties) as compared to the genetically and chemically modified constructs. Secondly, the genetically and chemically modified constructs resulted in Gd^{3+} ions that are anchored to the protein capsid in a more flexible manner as compared to the endogenous binding site. These more flexible chelators negate much of the beneficial qualities of the slow rotational tumbling of the large protein cage structures.

Other studies chemically attached flexible Gd^{3+}-containing groups to the viral capsids; MS2, CPMV and Qβ (these capsids are similar in size to CCMV), which produced relaxivity values lower than the chemically modified CCMV-GdDOTA construct (Anderson et al. 2006; Prasuhn et al. 2007). Together these studies suggest that the relaxivity values improve with the use of shorter, more rigid Gd^{3+} linkers. Others have used hydroxypyridinone (HOPO)-based chelators to coordinate Gd^{3+}. In doing so, they took advantage of the higher number of ligand water molecules bound to Gd^{3+} and an ideal water exchange lifetime (Datta et al. 2008; Hooker et al. 2004). Also, their reaction scheme allowed for specific modification of the interior or the exterior of the MS2 viral capsid with GdHOPO. The results of

this analysis produced relaxivity values slightly lower than that of the CCMV-GdDOTA construct but higher than the other Gd/capsid-based systems studied to date (Anderson et al. 2006; Prasuhn et al. 2007). The fit of their results to theoretical models provided insight into the factors that are responsible for producing relaxivity in Gd^{3+} based systems.

Protein Cages for Targeted Therapeutic and Imaging Agent Delivery

One of our goals is to develop protein cage architectures that serve as cell-specific therapeutic and imaging-agent delivery systems. Targeted therapeutic delivery systems can enhance the effective dose at the site, such as a tumor, while decreasing general exposure to the drug and its associated side effects (Allen and Cullis 2004). Protein cage architectures have three surfaces (interior, subunit interface, and exterior) amenable to both genetic and chemical modification. Figure 2 depicts a schematic representation of how each surface can play a distinct role in the development of new targeted therapeutic and imaging agent delivery systems. The cage interior can house therapeutics, the subunit interface incorporates gadolinium (an MRI contrast agent) and the exterior presents cell-specific targeting ligands (such as peptides and antibodies).

Protein cages have many beneficial attributes that are useful in their development as targeted therapeutic and imaging agent delivery systems. Their size falls into the nanometer range shown to localize in tumors due to the enhanced permeability and retention effect (Allen and Cullis 2004; Hashizume et al. 2000; Maeda et al. 2000). Their multivalent nature enables the incorporation of multiple functionalities (including targeting peptides and imaging agents) on a single protein cage. They are malleable to both chemical and genetic manipulation and can be produced in heterologous expression systems (including bacterial, yeast, and baculoviral systems) (Allen et al. 2002; Brumfield et al. 2004; Flenniken et al. 2003; Ramsay et al. 2006; Wiedenheft et al. 2005). In addition, detailed atomic resolution structural information enables the rational design of genetic mutants with specific functions, including cell-specific targeting (Douglas et al. 2002b; Flenniken et al. 2003, 2006; Gillitzer et al. 2002; Liepold et al. 2007; Uchida et al. 2006).

The CCMV protein cage was utilized in our first example of encapsulation of an organic compound (Douglas and Young 1998). The gating properties of the CCMV cage (swollen confirmation at pH 6.5 or higher, closed confirmation below pH 6.5) were utilized for the entrapment of an organic polyanion, polyanetholesulphonic acid (Douglas and Young 1998). We have also genetically introduced a redox-dependant chemical switch for reversible gating of CCMV and demonstrated in vitro functionality (C. Crowley et al., unpublished data). In this variant of CCMV, cysteines were introduced at the quasi-threefold axis, resulting in a capsid that is in a compact, closed conformation under oxidizing conditions and undergoes a transition to an open conformation under reducing conditions (C. Crowley et al., unpublished data).

In addition to the entrapment of materials on the interior, the CCMV protein cage and its genetic variants have been chemically derivatized on both the exterior and interior surfaces (M.L. Flenniken et al., unpublished data; Gillitzer et al. 2002; Suci et al. 2007) (Fig. 8a, b). Initially, we chemically linked fluorescent molecules and a peptide to CCMV protein cage platforms (Gillitzer et al. 2002). Fluorescent reporter molecules are useful for detection and quantification of the extent of derivatization. The degree of labeling of different sites on the CCMV platforms was highly dependent on reaction conditions (M.L. Flenniken et al., unpublished data; Gillitzer et al. 2002).

The small Hsp cage (*Mj*Hsp) of *M. jannaschii* was also labeled with fluorescent molecules, illustrating that many protein platforms within our library of cages perform similarly as chemical building blocks (Flenniken et al. 2003). Although

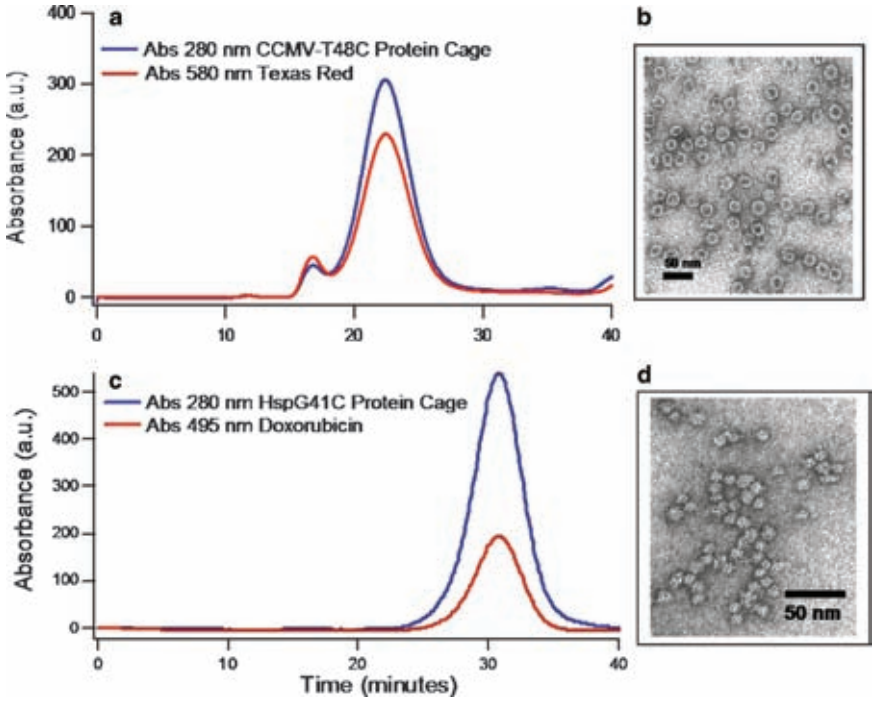

Fig. 8a–d Interiorly derivatized CCMV (T48C) and Hsp (G41C). **a** Size exclusion chromatography (SEC) elution profile of CCMV illustrating the co-elution of CCMV (T48C) protein cage (Abs 280 nm) and Texas Red (Abs 580 nm). **b** TEM of CCMV(T48C)-Texas red (stained with uranyl acetate). Scale bar, 50 nm. **c** SEC elution profile of Hsp (G41C) labeled with the (6-Maleimidocaproyl) hydrazone of doxorubicin (a chemotherapeutic agent), illustrating the co-elution of the Hsp protein cage (Abs 280) and doxorubicin (Abs 495). **d** TEM of HspG41C cages containing doxorubicin (stained with uranyl acetate). Scale bar, 50 nm. (Adapted from Flenniken et al. 2005)

similar in reactivity, the endogenous properties including structure, amino acid composition, size, pH stability, temperature stability, and solvent accessibility of each protein cage differs. These differences can be used to our advantage. The *Mj*Hsp cage as compared to CCMV is a much smaller (~12-nm exterior diameter), more solvent accessible protein cage assembled from 24 identical subunits. The *Mj*Hsp cage, like CCMV, is readily amenable to genetic modification. In order to chemically derivatize *Mj*Hsp in a spatially selective manner, we generated two mutants with either internally or externally exposed cysteine residues (G41C and S121C, respectively) and subsequently characterized their reactivities with activated fluorescent molecules (Flenniken et al. 2003). Protein architectures can be viewed as building blocks with a range of generic chemistry (e.g., thiol–maleimide coupling) that can be used to link reporter molecules and other compounds, including therapeutics. We demonstrated the selective attachment and release of a chemotherapeutic agent (doxorubicin) from the interior of a genetically modified *Mj*Hsp cage, HspG41C (Flenniken et al. 2005) (Fig. 8c, d). The advantage of this approach is that housing therapeutics within protein cages limits their bioavailability until their environmentally triggered release. We demonstrated pH-dependant release of doxorubicin from HspG41C under biologically relevant (lysosomal mimicking) conditions (Flenniken et al. 2005).

Another key component for the development of protein cage architectures as imaging and therapeutic agents is cell-specific targeting. In vivo application of the phage display library technique enabled the identification of peptides that bind specifically to the vasculature of particular organs as well as tumors (Arap et al. 1998a, 1998b, 2002; Pasqualini and Ruoslahti 1996a, 1996b; Pasqualini et al. 2000; Ruoslahti 2000). One of the most characterized of these targeting peptides is RGD-4C (CDCRGDCFC), which binds $\alpha_v\beta_3$ and $\alpha_v\beta_5$ integrins that are more prevalently expressed within tumor vasculature (Arap et al. 1998a; Brooks et al. 1994; Friedlander et al. 1995; Koivunen et al. 1995; Pasqualini et al. 1995). We incorporated RGD-4C and other targeting peptides on the exteriors of both *Mj*Hsp (HspG41C-RGD4C) and human H-chain ferritin (RGD4C-HFn) (Flenniken et al. 2006; Uchida et al. 2006). Fluorescein labeling of cell-specific targeted cages enables their visualization by epifluorescence microscopy. Using this approach, we demonstrated RGD-4C-mediated cell targeting of HspG41CRGD-4C cages in vitro (Fig. 9) (Flenniken et al. 2006). In addition to genetic incorporation, cell-specific targeting ligands, including antibodies and peptides, have also been chemically coupled to protein cage platforms (Chatterji et al. 2002, 2004b; Flenniken et al. 2006; Gillitzer et al. 2002; Medintz et al. 2005). For example, an anti-CD4 monoclonal antibody conjugated to fluorescently labeled HspG41C enabled targeting of $CD4^+$ lymphocytes within a population of splenocytes (Flenniken et al. 2006). The multivalent nature of protein cage architectures results in the presentation of multiple targeting ligands on their surfaces and may potentially aid in the interaction of these protein cages with many surfaces including receptors on a variety of cell types.

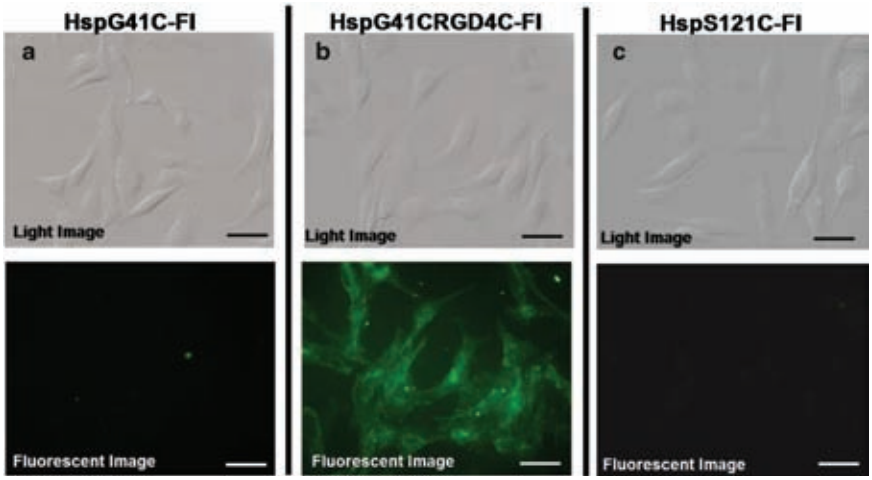

Fig. 9a–c Epifluorescence microscopy of C32 melanoma cells with Hsp cage-fluorescein conjugates. Cells were incubated with (**a**) nontargeted HspG41C-Fl cages with internally bound fluorescein, (**b**) tumor targeted HspG41CRGD4C-Fl cages and (**c**) nontargeted HspS121C-Fl cages with externally bound fluorescein. C32 melanoma cells grown on coverslips were incubated with Hsp cage-fluorescein conjugates and imaged by both light (*top*) and fluorescent microscopy (*bottom*). The fluorescein concentration for cage-cell incubations was 2.5 mM and all fluorescent images were taken at a standardized camera exposure time of 50 ms. Scale bar, 50 mm. (Flenniken et al. 2006)

Asymmetric Derivatization of Inherently Symmetric Protein Cage Architectures

High symmetry is an inherent property of protein cage architectures that are typically assembled from multiple copies of a single protein. While symmetric ligand presentation is often desired, we have also developed approaches for the asymmetric presentation of ligands on a protein cage while maintaining their structure (Gillitzer et al. 2006; Klem et al. 2003). In the first approach, one face of a CCMV capsid (genetic variant A163C with exteriorly exposed thiol groups) was reversibly bound through exposed thiols to an activated resin, followed by the passivation of the remaining thiols with iodoacetic acid and subsequent elution of the cages (Klem et al. 2003). The resulting CCMV capsids, with reactive thiol groups present on a single face, bound a solid gold substrate in an ordered fashion resulting in a 2D monolayer of virus particles (Klem et al. 2003). A second symmetry-breaking approach capitalized on the subunit assembly and disassembly process of protein cages to generate CCMV populations with asymmetric presentation of ligands (Gillitzer et al. 2006). Two populations of CCMV capsids differentially modified (with either biotin or digoxigenin) were disassembled into subunits and subsequently combined (in varying stoichiometries) and reassembled, resulting

in dual functionalized capsids (Gillitzer et al. 2006). The introduction of dual functionality to a single protein cage platform is a step toward developing cages with multiple functionalities. Ultimately, the goal is to control the number and spatial arrangement of ligands on the cage, independent of the symmetry of the underlying architecture.

In Vivo Study of Protein Cage-Mediated Materials for Medical Applications

As described in the previous sections, protein cages have the potential as nanoplatforms in medical applications. However, it is critical to investigate biocompatibility and biodistribution of the protein cage particles in vivo before proceeding to preclinical and clinical studies. We have examined biodistribution of two different protein cages, CCMV and *Mj*Hsp and demonstrated both cages shows similar broad distribution in most tissues and organs and no obvious toxicity after a single injection (Kaiser et al. 2007). These results indicate that protein-cage-based nanoparticles are biocompatible and could be utilized as in vivo biomedical materials. On the basic of this knowledge, we have been developing iron-oxide-encapsulated protein cages for MRI contrast agents (M. Uchida et al., unpublished data).

Manchester and co-workers have studied the biocompatibility of another viral protein cage, CPMV, and revealed that it also has the potential to serve as a nontoxic platform in medical use (Rae et al. 2005; Singh et al. 2007). Furthermore, they have demonstrated that fluorescently labeled CPMV is internalized in vascular endothelial cells and can be used as an imaging probe to visualize the vasculature and blood flow in living mice (Lewis et al. 2006).

Introduction of Multiple Functionalities on a Single Protein Cage Architecture

Thus far, we have demonstrated functionalities including biomimetic mineralization, chemical derivatization with both fluorescent and therapeutic molecules, genetic and chemical introduction of cell-specific targeting ligands, genetic incorporation of metal coordinating peptides, and chemical linkage of gadolinium chelators on protein cage architectures. In addition, we have shown that protein cages with cell-specific targeting capabilities can simultaneously be chemically modified with fluorescent molecules, therefore creating a cage with both cell-targeting and imaging capabilities (Flenniken et al. 2006). The next phase of our efforts toward the development of protein cage architectures as nanomaterials for bioengineering and biomedicine is focused on the incorporation of multiple modalities on a single protein cage platform. Ultimately, the utility of these materials for medical applications must be evaluated in vivo and these studies are currently in progress.

Conclusion

The use of protein cage architectures of viral and nonviral origin as nanomaterials with applications in biomedicine and biotechnology provides a number of unique advantages. Their biological origin makes them both amenable to genetic modification and large-scale production. Genetic modification enables the site-specific introduction of chemical and/or structural functionality onto highly symmetric protein cage platforms. The presence of reactive functional groups also allows a chemical approach to the attachment and presentation of both organic and inorganic ligands. This structural and functional plasticity allows many protein cage systems within our library to be engineered and redesigned for specific applications in materials science, catalysis, and biomedicine. In addition, the ability to break the inherent symmetry of the cage-like architectures holds promise for very precise control over placement and presentation of functionalized ligands on these templates. The chemistry presented here is fundamentally biomimetic, where lessons learned from how biological systems deal with issues of spatial control and assembly have been applied to purely or partially synthetic systems. While there are certainly competing approaches, the use of protein cage architectures for nanomaterials synthesis is both an exciting and potentially fruitful arena.

References

Ackermann HW (2001) Frequency of morphological phage descriptions in the year 2000. Brief review. Arch Virol 146:843–857

Allen TM, Cullis PR (2004) Drug delivery systems: entering the mainstream. Science 303:1818–1822

Allen M, Willits D, Mosolf J, Young M, Douglas T (2002) Protein cage constrained synthesis of ferrimagnetic iron oxide nanoparticles. Adv Mater 14:1562–1565

Allen M, Willits D, Young M, Douglas T (2003) Constrained synthesis of cobalt oxide nanomaterials in the 12-subunit protein cage from *Listeria innocua*. Inorg Chem 42:6300–6305

Allen MA, Bulte JWM, Liepold L, Basu G, Zywicke HA, Frank JA, Young M, Douglas T (2005) Paramagnetic viral nanoparticles as potential high-relaxivity magnetic resonance contrast agents. Magn Reson Med 54:807–812

Anderson EA, Isaacman S, Peabody DS, Wang EY, Canary JW, Kirshenbaum K (2006) Viral nanoparticles donning a paramagnetic coat: conjugation of MRI contrast agents to the MS2 capsid. Nano Lett 6:1160–1164

Arap W, Pasqualini R, Ruoslahti E (1998a) Cancer treatment by targeted drug delivery to tumor vasculature in a mouse model. Science 279:377–380

Arap W, Pasqualini R, Ruoslahti E (1998b) Chemotherapy targeted to tumor vasculature. Curr Opin Oncol 10:560–565

Arap W, Haedicke W, Bernasconi M, Kain R, Rajotte D, Krajewski S, Ellerby HM, Bredesen DE, Pasqualini R, Ruoslahti E (2002) Targeting the prostate for destruction through a vascular address. Proc Natl Acad Sci U S A 99:1527–1531

Basu G, Allen M, Willits D, Young M, Douglas T (2003) Metal binding to cowpea chlorotic mottle virus using terbium(III) fluorescence. J Biol Inorg Chem 8:721–725

Belcher A, Flynn C, Whaley S, Mao CB, Gooch E (2001) Biomolecular recognition and control of nano magnetic and semiconductor materials. Abstr Papers Chemical Soc 222:53-POLY

Brooks PC, Montgomery AM, Rosenfeld M, Reisfeld RA, Hu T, Klier G, Cheresh DA (1994) Integrin alpha v beta 3 antagonists promote tumor regression by inducing apoptosis of angiogenic blood vessels. Cell 79:1157–1164

Brumfield S, Willits D, Tang L, Johnson JE, Douglas T, Young M (2004) Heterologous expression of modified Cowpea chlorotic mottle bromovirus coat protein results in the assembly of protein cages with altered architectures and function. J Gen Virol 85:1049–1053

Bulte JWM, Douglas T, Mann S, Frankel RB, Moskowitz BM, Brooks RA, Baumgarner CD, Vymazal J, Frank JA (1994a) Magnetoferritin: biomineralization as a novel approach in the design of iron oxide-based MR contrast agents. Inv Rad 29:S214–S216

Bulte JWM, Douglas T, Mann S, Frankel RB, Moskowitz BM, Brooks RA, Baumgarner CD, Vymazal J, Strub M-P, Frank JA (1994b) Magnetoferritin: characterization of a novel superparamagnetic MR contrast agent. J Magn Res Imaging 4:497–505

Bulte CJ, White O, Olsen GJ, Zhou L, Fleischmann RD, Sutton GG, Blake JA, FitzGerald LM, Clayton RA, Gocayne JD, Kerlavage AR, Dougherty BA, Tomb JF, Adams MD, Reich CI, Overbeek R, Kirkness EF, Weinstock KG, Merrick JM, Glodek A, Scott JL, Geoghagen NS, Venter JC (1996) Complete genome sequence of the methanogenic archaeon *Methanococcus jannaschii*. Science 273:1058–1073

Bulte JWM, Douglas T, Witwer B, Zhang SC, Strable E, Lewis BK, Zywicke H, Miller B, van Gelderen P, Moskowitz BM, Duncan ID, Frank JA (2001) Magnetodendrimers allow endosomal magnetic labeling and in vivo tracking of stem cells. Nat Biotechnol 19:1141–1147

Burritt JB, Bond CW, Doss KW, Jesaitis AJ (1996) Filamentous phage display of oligopeptide libraries. Anal Biotechnol. 238:1–13

Chasteen ND, Harrison PM (1999) Mineralization in ferritin: an efficient means of iron storage. J Struct Biol 126:182–194

Chatterji A, Burns LL, Taylor SS, Lomonossoff GP, Johnson JE, Lin T, Porta C (2002) Cowpea mosaic virus: from the presentation of antigenic peptides to the display of active biomaterials. Intervirology 45:362–370

Chatterji A, Ochoa WF, Paine M, Ratna BR, Johnson JE, Lin T (2004a) New addresses on an addressable virus nanoblock; uniquely reactive Lys residues on cowpea mosaic virus. Chem Biol 11:855–863

Chatterji A, Ochoa W, Shamieh L, Salakian SP, Wong SM, Clinton G, Ghosh P, Lin T, Johnson JE (2004b) Chemical conjugation of heterologous proteins on the surface of Cowpea mosaic virus. Bioconjug Chem 15:807–813

Chatterji A, Ochoa WF, Ueno T, Lin T, Johnson JE (2005) A virus-based nanoblock with tunable electrostatic properties. Nano Lett 5:597–602

Datta A, Hooker JM, Botta M, Francis MB, Aime S, Raymond KN (2008) High relaxivity gadolinium hydroxypyridonate-viral capsid conjugates: nanosized MRI contrast agents. 1. J Am Chem Soc 130:2546–2552

Douglas T (1996) Biomimetic synthesis of nanoscale particles in organized protein cages. In: Mann S (ed) Biomimetic approaches in materials science. VCH, New York, pp 91–115

Douglas T, Mann S (1995) Biomolecules in the synthesis of inorganic solids. In: Meyers RA (ed) Molecular biology and biotechnology. VCH, New York, pp 466–469

Douglas T, Ripoll D (1998) Electrostatic gradients in the iron storage protein ferritin. Protein Sci 7:1083–1091

Douglas T, Young M (1998) Host-guest encapsulation of materials by assembled virus protein cages. Nature (London) 393:152–155

Douglas T, Young M (1999) Virus particles as templates for materials synthesis. Adv Mater 11:679–681

Douglas T, Stark VT (2000) Nanophase cobalt oxyhydroxide mineral synthesized within the protein cage of ferritin. Inorg Chem 39:1828–1830

Douglas T, Allen M, Young M (2002a) Self-assembling protein cage systems and applications in nanotechnology. In: Fahnstock SR, Steinbuchel A (eds) Polyamides and complex proteinaceous materials I, Vol. 7. Wiley-VCH, Weinheim, p 517

Douglas T, Strable E, Willits D, Aitouchen A, Libera M, Young M (2002b) Protein engineering of a viral cage for constrained nano-materials synthesis. Adv Mater 14:415–418
Douglas T, Allen M, Klem M, Gilmore K, Idzerda Y, Young M (2004) Engineered protein cages for nanomaterials. Abstr Papers Am Chem Soc 227:U519–U519
Endo M, Fujitsuka M, Majima T (2007) Porphyrin light-harvesting arrays constructed in the recombinant tobacco mosaic virus scaffold. Chem Eur J 13:8660–8666
Ensign D, Young MJ, Douglas T (2004) Photocatalytic synthesis of copper colloids from Cu(II) by the ferrihydrite core of ferritin. Inorg Chem 43:3441–3446
Flenniken ML, Willits DA, Brumfield S, Young MJ, Douglas T (2003) The small heat shock protein cage from *Methanococcus jannaschii* is a versatile nanoscale platform for genetic and chemical modification. Nano Lett 3:1573–1576
Flenniken ML, Allen M, Young M, Douglas T (2004) Viruses as host assemblies. In: Encyclopedia of supramolecular chemistry. Steed AJW (ed) NMarcel Dekker, ew York City, pp 1563–1568
Flenniken ML, Liepold LO, Crowley BE, Willits DA, Young MJ, Douglas T (2005) Selective attachment and release of a chemotherapeutic agent from the interior of a protein cage architecture. Chem Commun (Camb) 447–449
Flenniken ML, Willits DA, Harmsen AL, Liepold LO, Harmsen AG, Young MJ, Douglas T (2006) Melanoma and lymphocyte cell-specific targeting incorporated into a heat shock protein cage architecture. Chem Biol 13:161–170
Friedlander M, Brooks PC, Shaffer RW, Kincaid CM, Varner JA, Cheresh DA (1995) Definition of two angiogenic pathways by distinct alpha v integrins. Science 270:1500–1502
Gillitzer E, Willits D, Young M, Douglas T (2002) Chemical modification of a viral cage for multivalent presentation. Chem Commun (Camb) 2390–2391
Gillitzer E, Succi P, Young M, Douglas T (2006) Controlled ligand display on a symmetrical protein-cage architecture through mixed assembly. Small 2:962–966
Harrison PM, Arosio P (1996) The ferritins: molecular properties, iron storage function and cellular regulation. Biochim Biophys Acta 1275:161–203
Harrison PM, Banyard SH, Hoare RJ, Russell SM, Treffry A (1976) The structure and function of ferritin. Ciba Found Symp 19–40
Hashizume H, Baluk P, Morikawa S, McLean JW, Thurston G, Roberge S, Jain RK, McDonald DM (2000) Openings between defective endothelial cells explain tumor vessel leakiness. Am J Pathol 156:1363–1380
Hikono T, Matsumura T, Miura A, Uraoka Y, Fuyuki T, Takeguchi M, Yoshii S, Yamashita I (2006) Electron confinement in a metal nanodot monolayer embedded in silicon dioxide produced using ferritin protein. Appl Phys Lett 88:023108
Hooker JM, Kovacs EW, Francis MB (2004) Interior surface modification of bacteriophage MS2. J Am Chem Soc 126:3718–3719
Hooker JM, Datta A, Botta M, Raymond KN, Francis MB (2007) Magnetic resonance contrast agents from viral capsid shells: a comparison of exterior and interior cargo strategies. Nano Lett 7:2207–2210
Hosein HA, Strongin DR, Allen M, Douglas T (2004) Iron and cobalt oxide and metallic nanoparticles prepared from ferritin. Langmuir 20:10283–10287
Ichikawa K, Uraoka Y, Punchaipetch P, Yano H, Hatayama T, Fuyuki T, Yamashita I (2007) Low-temperature polycrystalline silicon thin film transistor flash memory with ferritin. Jpn J Appl Phys 46:L804–L806
Iwahori K, Yoshizawa K, Muraoka M, Yamashita I (2005) Fabrication of ZnSe nanoparticles in the apoferritin cavity by designing a slow chemical reaction system. Inorg Chem 44:6393–6400
Johnson JE, Speir JA (1997) Quasi-equivalent viruses: a paradigm for protein assemblies. J Mol Biol 269:665–675
Kaiser CR, Flenniken ML, Gillitzer E, Harmsen AL, Harmsen AG, Jutila MA, Douglas T, Young MJ (2007) Biodistribution studies of protein cage nanoparticles demonstrate broad tissue distribution and rapid clearance in vivo. Int J Nanomed 2:715–733

Kawashita M, Tanaka M, Kokubo T, Inoue Y, Yao T, Hamada S, Shinjo T (2005) Preparation of ferrimagnetic magnetite microspheres for in situ hyperthermic treatment of cancer. Biomater 26:2231–2238

Kim I, Hosein HA, Strongin DR, Douglas T (2002) Photochemical reactivity of ferritin for Cr(VI) reduction. Chem Mater 14:4874–4879

Kim KK, Kim R, Kim SH (1998a) Crystal structure of a small heat-shock protein. Nature 394:595–599

Kim KK, Yokota H, Santoso S, Lerner D, Kim R, Kim SH (1998b) Purification, crystallization, and preliminary X-ray crystallographic data analysis of small heat shock protein homolog from *Methanococcus jannaschii*, a hyperthermophile. J Struct Biol 121:76–80

Klem MT, Willits D, Young M, Douglas T (2003) 2-D array formation of genetically engineered viral cages on Au surfaces and imaging by atomic force microscopy. J Am Chem Soc 125:10806–10807

Klem M, Willits D, Solis DJ, Belcher A, Young M, Douglas T (2005a) Bio-inspired synthesis of protein-encapsulated CoPt nanoparticles. Adv Funct Mater 15:1489–1494

Klem M, Young M, Douglas T (2005b) Biomimetic magnetic nanoparticles. Mater Today 8:28–37

Klem MT, Mosolf J, Young M, Douglas T (2008) Photochemical mineralization of europium titanium, iron oxyhydroxide nanoparticles in the ferritin protein cage. Inorg Chem 47:2237–2239

Koivunen E, Wang B, Ruoslahti E (1995) Phage libraries displaying cyclic peptides with different ring sizes: ligand specificities of the RGD-directed integrins. Biotechnology (N Y) 13:265–270

Kramer RM, Li C, Carter DC, Stone MO, Naik RR (2004) Engineered protein cages for nanomaterial synthesis. J Am Chem Soc 126:13282–13286

Le Clainche L, Plancque G, Amekraz B, Moulin C, Pradines-Lecomte C, Peltier G, Vita C (2003) Engineering new metal specificity in EF-hand peptides. J Biol Inorg Chem 8:334–340

Lewis JD, Destito G, Zijlstra A, Gonzalez MJ, Quigley JP, Manchester M, Stuhlmann H (2006) Viral nanoparticles as tools for intravital vascular imaging. Nat Med 12:354–360

Liepold LO, Willits D, Oltrogge L, Allen M, Young M, Douglas T (2007) Viral capsids as MRI contrast agents. Magn Reson Med 58:871–879

Luderer AA, Borrelli NF, Panzarino JN, Mansfield GR, Hess DM, Brown JL, Barnett EH, Hahn EW (1983) Glass-ceramic-mediated, magnetic-field-induced localized hyperthermia: response of a murine mammary carcinoma. Radiat Res 94:190–198

Maeda H, Wu J, Sawa T, Matsumura Y, Hori K (2000) Tumor vascular permeability and the EPR effect in macromolecular therapeutics: a review. J Control Release 65:271–284

Maeder DL, Weiss RB, Dunn DM, Cherry JL, Gonzalez JM, DiRuggiero J, Robb FT (1999) Divergence of the hyperthermophilic archaea *Pyrococcus furiosus* and *P. horikoshii* inferred from complete genomic sequences. Genetics 152:1299–1305

Mao C, Flynn CE, Hayhurst A, Sweeney R, Qi J, Georgiou G, Iverson B, Belcher AM (2003) Viral assembly of oriented quantum dot nanowires. Proc Natl Acad Sci U S 100:6946–6951

Mao C, Solis DJ, Reiss BD, Kottmann ST, Sweeney RY, Hayhurst A, Georgiou G, Iverson B, Belcher AM (2004) Virus-based toolkit for the directed synthesis of magnetic and semiconducting nanowires. Science 303:213–217

Matsui T, Matsukawa N, Iwahori K, Sano KI, Shiba K, Yamashita I (2007) Direct production of a two-dimensional ordered array of ferritin-nanoparticles on a silicon substrate. Jpn J Appl Phys 46:L713–L715

Medintz IL, Sapsford KE, Konnert JH, Chatterji A, Lin T, Johnson JE, Mattoussi H (2005) Decoration of discretely immobilized cowpea mosaic virus with luminescent quantum dots. Langmuir 21:5501–5510

Miller RA, Presley AD, Francis MB (2007) Self-assembling light-harvesting systems from synthetically modified tobacco mosaic virus coat proteins. J Am Chem Soc 129:3104–3109

Miura A, Hikono T, Matsumura T, Yano H, Hatayama T, Uraoka Y, Fuyuki T, Yoshii S, Yamashita I (2006) Floating nanodot gate memory devices based on biomineralized inorganic nanodot array as a storage node. Jpn J Appl Phys 45:L1–L3

Narberhaus F (2002) Alpha-crystallin-type heat shock proteins: socializing minichaperones in the context of a multichaperone network. Microbiol Mol Biol Rev 66:64–93

Nkere UU, Walter NM, Nikandrov VV, Gratzel CK, Moser JE, Gratzel MJ (1997) Light induced redox reactions involving mammalian ferritin as a photocatalyst. Photochem Photobiol B 41:83–89

Parker MJ, Allen MA, Ramsay B, Klem MT, Young M, Douglas T (2008) Expanding the temperature range of biomimetic synthesis using a ferritin from the hyperthermophile *Pyrococcus furiosus*. Chem Mater 20:1541–1547

Pasqualini R, Ruoslahti E (1996a) Organ targeting in vivo using phage display peptide libraries. Nature 380:364–366

Pasqualini R, Ruoslahti E (1996b) Tissue targeting with phage peptide libraries. Mol Psychiatry 1:423

Pasqualini R, Koivunen E, Ruoslahti E (1995) A peptide isolated from phage display libraries is a structural and functional mimic of an RGD-binding site on integrins. J Cell Biol 130:1189–1196

Pasqualini R, Koivunen E, Kain R, Lahdenranta J, Sakamoto M, Stryhn A, Ashmun RA, Shapiro LH, Arap W, Ruoslahti E (2000) Aminopeptidase N is a receptor for tumor-homing peptides and a target for inhibiting angiogenesis. Cancer Res 60:722–727

Prasuhn DE, Yeh RM, Obenaus A, Manchester M, Finn MG (2007) Viral MRI contrast agents: coordination of Gd by native virions and attachment of Gd complexes by azide-alkyne cycloaddition. Chem Comm 28:1269–1271

Rae CS, Khor IW, Wang Q, Destito G, Gonzalez MJ, Singh P, Thomas DM, Estrada MN, Powell E, Finn MG, Manchester M (2005) Systemic trafficking of plant virus nanoparticles in mice via the oral route. Virology 343:224–235

Raja KS, Wang Q, Finn MG (2003a) Icosahedral virus particles as polyvalent carbohydrate display platforms. Chembiochem 4:1348–1351

Raja KS, Wang Q, Gonzalez MJ, Manchester M, Johnson JE, Finn MG (2003b) Hybrid virus-polymer materials. 1. Synthesis and properties of PEG-decorated cowpea mosaic virus. Biomacromolecules 4:472–476

Ramsay B, Wiedenheft B, Allen M, Gauss GH, Lawrence CM, Young M, Douglas T (2006) Dps-like protein from the hyperthermophilic archaeon *Pyrococcus furiosus*. J Inorg Biochem 100:1061–1068

Reddy VS, Nataraja, P, Okerberg B, Li K, Damodaran KV, et al (2001) Virus Partilce Explorer (VIPER), a website for virus capsid structures and their computational analyses. J Virol 75:11943–11947

Rice G, Stedman K, Snyder J, Wiedenheft B, Willits D, Brumfield S, McDermott T, Young MJ (2001) Viruses from extreme thermal environments. Proc Natl Acad Sci U S A 98:13341–13345

Rice G, Tang L, Stedman K, Roberto F, Sphuler J, Gillitzer E, Johnson JE, Douglas T, Young M (2004) The structure of a thermophilic archaeal virus shows a double-stranded DNA viral capsid type that spans all three domains of life. Proc Natl Acad Sci U S A 101:7716–7720

Ruoslahti E (2000) Targeting tumor vasculature with homing peptides from phage display. Semin Cancer Biol 10:435–442

Schlick TL, Ding Z, Kovacs EW, Francis MB (2005) Dual-surface modification of the tobacco mosaic virus. J Am Chem Soc 127:3718–3723

Schneemann A, Young MJ (2003) Viral assembly using heterologous expression systems and cell extracts. Adv Protein Chem 64:1–36

Scott JK, Smith GP (1990) Searching for peptide ligands with an epitope library. Science 249:386–390

Seeman NC, Belcher AM (2002) Emulating biology: Building nanostructures from the bottom up. Proc Natl Acad Sci U S A 99:6451–6455

Singh P, Prasuhn D, Yeh RM, Destito G, Rae CS, Osborn K, Finn MG, Manchester M (2007) Bio-distribution, toxicity and pathology of cowpea mosaic virus nanoparticles in vivo. J Control Release 120:41–50

Smith GP, Petrenko VA (1997) Phage display. Chem Rev 97:391–410
Snyder JC, Stedman K, Rice G, Wiedenheft B, Spuhler J, Young MJ (2003) Viruses of hyperthermophilic Archaea. Res Microbiol 154:474–482
Speir JA, Munshi S, Wang G, Baker TS, Johnson JE (1995) Structures of the native and swollen forms of cowpea chlorotic mottle virus determined by X-ray crystallography and cryo-electron microscopy. Structure 3:63–78
Stefanini S, Cavallo S, Montagnini B, Chiancone E (1999) Incorporation of iron by the unusual dodecameric ferritin from *Listeria innocua*. Biochem J 338:71–75
Strable E, Johnson JE, Finn MG (2004) Natural nanochemical building blocks: icosahedral virus particles organized by attached oligonucleotides. Nano Lett 4:1385–1389
Su M, Cavallo S, Stefanini S, Chiancone E, Chasteen ND (2005) The so-called *Listeria innocua* ferritin is a Dps protein. Iron incorporation, detoxification, DNA protection properties. Biochemistry 44:5572–5578
Suci PA, Berglund DL, Liepold L, Brumfield S, Pitts B, Davison W, Oltrogge L, Hoyt KO, Codd S, Stewart PS, Young M, Douglas T (2007) High-density targeting of a viral multifunctional nanoplatform to a pathogenic, biofilm-forming bacterium. Chem Biol 14:387–398
Uchida M, Flenniken ML, Allen M, Willits DA, Crowley BE, Brumfield S, Willis AF, Jackiw L, Jutila M, Young MJ, Douglas T (2006) Targeting of cancer cells with ferrimagnetic ferritin cage nanoparticles. J Am Chem Soc 128:16626–16633
Varpness Z, Peters JW, Young M, Douglas T (2005) Biomimetic synthesis of a H2 catalyst using a protein cage architecture. Nano Lett 5:2306–2309
Wang Q, Kaltgrad E, Lin T, Johnson JE, Finn MG (2002a) Natural supramolecular building blocks. Wild-type cowpea mosaic virus. Chem Biol 9:805–811
Wang Q, Lin T, Johnson JE, Finn MG (2002b) Natural supramolecular building blocks. Cysteine-added mutants of cowpea mosaic virus. Chem Biol 9:813–819
Wang Q, Lin TW, Tang L, Johnson JE, Finn MG (2002c) Icosahedral virus particles as addressable nanoscale building blocks. Angew Chem Int Ed. 41:459–462
Whaley SR, English DS, Hu EL, Barbara PF, Belcher AM (2000) Selection of peptides with semiconductor binding specificity for directed nanocrystal assembly. Nature 405:665–668
Wiedenheft B, Mosolf J, Willits D, Yeager M, Dryden KA, Young M, Douglas T (2005) From the cover: an archaeal antioxidant: characterization of a Dps-like protein from *Sulfolobus solfataricus*. Proc Natl Acad Sci U S A 102:10551–10556
Wikipedia (2005) Wikipedia Free Encyclopedia, Wikipedia
Yamada K, Yoshii S, Kumagai S, Miura A, Uraoka Y, Fuyuki T, Yamashita I (2007) Effects of dot density and dot size on charge injection characteristics in nanodot array produced by protein supramolecules. Jpn J Appl Phys 46:7549–7553
Yang XK, Chiancone E, Stefanini S, Ilari A, Chasteen ND (2000) Iron oxidation and hydrolysis reactions of a novel ferritin from *Listeria innocua*. Biochem J 349:783–786
Zhao X, Fox JM, Olson NH, Baker TS, Young MJ (1995) In vitro assembly of cowpea chlorotic mottle virus from coat protein expressed in *Escherichia coli* and in vitro-transcribed viral cDNA. Virology 207:486–494

http://www.springer.com/978-3-540-69376-5

Viruses and Nanotechnology
Manchester, M.; Steinmetz, N.F. (Eds.)
2009, X, 147 p., Hardcover
ISBN: 978-3-540-69376-5